Optical Response of Relativistic Electrons in the Polar BiTeI Semiconductor

J. S. Lee,[1,*] G. A. H. Schober,[2,3] M. S. Bahramy,[4] H. Murakawa,[5] Y. Onose,[2,5] R. Arita,[2,4] N. Nagaosa,[2,4] and Y. Tokura[1,2,4,5]

[1]*Department of Applied Physics and Quantum Phase Electronics Center (QPEC), University of Tokyo, Tokyo 113-8656, Japan*
[2]*Department of Applied Physics, University of Tokyo, Tokyo 113-8656, Japan*
[3]*Institut für Theoretische Physik, Universität Heidelberg, D-69120 Heidelberg, Germany*
[4]*Correlated Electron Research Group (CERG) and Cross-Correlated Materials Research Group (CMRG), ASI, RIKEN, Wako 351-0198, Japan*
[5]*Multiferroics Project, ERATO, Japan Science and Technology Agency (JST), Tokyo 113-8656, Japan*

(Received 28 February 2011; published 9 September 2011)

The transitions between the spin-split bands by spin-orbit interaction are relevant to many novel phenomena such as the resonant dynamical magnetoelectric effect and the spin Hall effect. We perform optical spectroscopy measurements combined with first-principles calculations to study these transitions in the recently discovered giant bulk Rashba spin-splitting system BiTeI. Several novel features are observed in the optical spectra of the material including a sharp edge singularity due to the reduced dimensionality of the joint density of states and a systematic doping dependence of the intraband transitions between the Rashba-split branches. These confirm the bulk nature of the Rashba-type splitting in BiTeI and manifest the relativistic nature of the electron dynamics in a solid.

DOI: 10.1103/PhysRevLett.107.117401 PACS numbers: 78.20.Bh, 71.18.+y, 71.70.Ej

The relativistic spin-orbit interaction (SOI) of electrons in solids has attracted recent intense interest in the fields of spintronics and multiferroics. The SOI can be taken into account by defining the pseudospin by a unitary transformation $U(k)$ when the time-reversal symmetry combined with the inversion (I) symmetry protects the double degeneracy at each k point. In this case, most of the physical properties of the spin-orbit coupled system are analogous to those without the SOI because the role of spin is mostly played by the pseudospin. In the absence of I symmetry, in contrast, the double degeneracy is generally lifted except at the time-reversal invariant k points, i.e., k and $-k$ being equivalent. This so-called spin splitting of the band leads to various novel phenomena such as the coupling between spin and current (Galvanic effect) [1–3] and noncentrosymmetric superconductivity [4]. The most representative SOI in the absence of I symmetry is the Rashba interaction [5] as given by $H_R = \lambda \vec{e}_z \cdot (\vec{s} \times \vec{p})$, where $\vec{e}_z$ is the direction of the potential gradient which breaks I symmetry and $\vec{s}$ and $\vec{p}$ are the spin and momentum operators, respectively. This interaction has been experimentally demonstrated for the two-dimensional electrons at the interface of GaAs system, where the coupling constant λ can be controlled by the gate voltage [6]. Also, the interface electrons in the oxides system offer another laboratory to study the Rashba Hamiltonian including the superconductivity [7,8]. Although the transport properties can be studied in these two-dimensional systems, other interesting quantities such as the magnetic susceptibility and optical conductivity can hardly be studied there. Therefore, the three-dimensional materials with simple band structure as described by the Rashba interaction have been searched for to study its novel phenomena as *bulk* properties. Especially, the transitions between the spin-split bands due to the SOI are of particular interest because they are relevant to the resonance-enhanced magnetoelectric effect and the spin Hall effect [9].

Recently, BiTeI, which lacks I symmetry and has a strong SOI due to Bi atoms, has been revisited from this viewpoint. An angle-resolved photoemission spectroscopy experiment by Ishizaka *et al.* [10] clearly shows that the band structure is described by the Rashba interaction near the conduction band minimum with a large spin splitting of the order of 0.4 eV at the outer Fermi surface. Moreover, the Rashba-split conduction band minimum is found to be by nearly $k_0 = \pm 0.05$ Å^{-1} shifted from the high symmetry point A $(0, 0, \pi)$ in the Brillouin zone. Such a large level of Rashba spin splitting lies among the highest reported so far [10,11]. While these results were found to be in excellent agreement with first-principles calculations [10,12], the high surface sensitivity of angle-resolved photoemission spectroscopy left the fundamental question unclear whether the giant Rashba spin splitting is really a bulk property or it originates from structurally distorted surface states.

In this Letter, we present a combined experimental and theoretical study on the dynamics of relativistic electrons in BiTeI by bulk-sensitive optical spectroscopy. The spin splitting by Rashba interaction leads to several unique features of the optical spectra including the sharp edge singularity due to the reduced dimensionality of the joint density of states and systematic change of the intraband or interband transitions between the Rashba-split branches

with carrier doping. These confirm the bulk nature of the Rashba-type splitting in BiTeI and, furthermore, manifest the relativistic nature of the electrons in a solid.

High-quality single crystalline samples were grown by the Bridgman method. Control of the carrier concentration (band filling) was attempted by doping Ag, Cu, and Mn as well as by changing the composition ratio between Te and I. In this work, we present the results for five samples with the carrier densities $n \simeq 0.2$, 0.4 (sample P), 3.5, 4.0 (sample Q), and $7.0 \times 10^{19}/\mathrm{cm}^3$ (sample R), which were determined by the Hall measurement. We have performed the optical measurement of reflectivity spectra (and transmittance spectra for some thin specimens) on the cleaved surface of the ab plane by using the Fourier-transform spectrometer and the grating-type spectrometer covering a wide spectral range from about 10 meV to 40 eV. The optical conductivity was derived through the Kramers-Kronig transformation.

In a BiTeI crystal, the Bi^{3+} ion, Te^{2-} ion, and I^- ion stack along the c axis forming a layered polar crystal (space group $P3m1$) as displayed in Fig. 1(a). In particular, the presence of a strong SOI of Bi drives the bands to split, depending on their spin states. Within each layer, Bi acts as a cation giving its outer $6p$ electrons to fill up Te-$5p$ and I-$5p$ states. Accordingly, the conduction (valence) bands above (below) the Fermi level (E_F) are dominated by Bi-$6p$ (Te-$5p$ and I-$5p$) states. The corresponding band structure for the highest valence and lowest conduction bands along the H-A-L direction is shown in Fig. 1(b). For both sets of bands, the figure clearly indicates a break in the spin degeneracy at any k point except for the A point, where the spin degeneracy is enforced by time-reversal symmetry. Accordingly, the spin splitting appears to be fully ruled by a Rashba-type interaction. A more detailed analysis reveals that the band dispersions are mainly two-dimensional within the plane encompassing A, H, and L points; however, one should not ignore a rather mild dispersion along $\Gamma - A$ [10]. The latter is expected to be due to a weak interaction between the consecutive Te-Bi-I layers along the c axis.

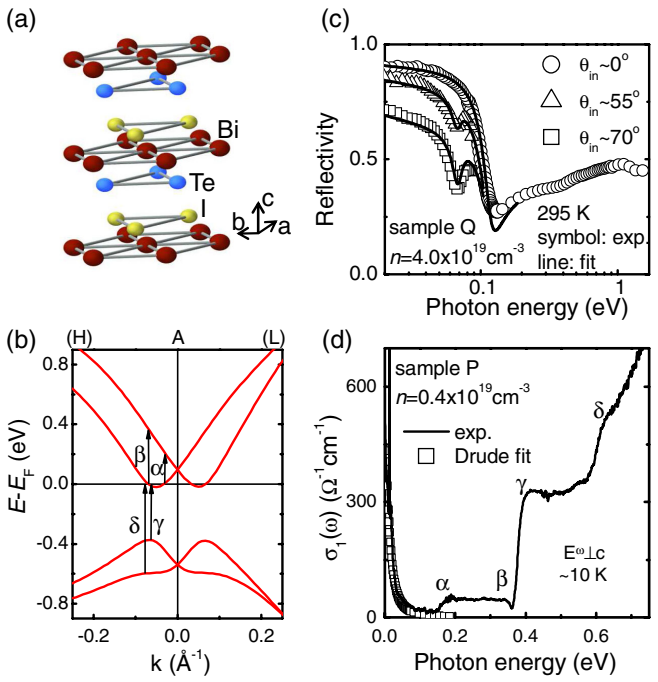

FIG. 1 (color online). (a) Crystal structure of BiTeI. (b) Band dispersion near the A point toward the H and L directions. The energy level is referenced to the Fermi level (E_F), which represents the case of the sample P with the carrier density of about $0.4 \times 10^{19}/\mathrm{cm}^3$. The possible optical transitions are indicated by arrows with an index of α, β, γ, and δ. (c) Reflectivity spectra for the sample Q obtained in different incidence angles θ_{in}. (d) Optical conductivity spectra for the sample P obtained with the light polarization (E^{ω}) directed normal to the c axis. Open squares indicate the fitting curve for the coherent excitation based on the simple Drude model.

The low dimensionality of the electronic structure can be revealed by the anisotropic optical response in the far-infrared region. Figure 1(c) shows the reflectivity spectra obtained with different incidence angles θ_{in} for the sample Q. In the near-normal incidence ($\theta_{\mathrm{in}} \simeq 0°$), the reflectivity in the low-energy region is dominated by the contribution from the free carriers, and it shows a dip structure around 0.13 eV corresponding to the plasma edge of the free carriers in the ab plane $\omega^*_{p,ab}$, which is related to n and the free carrier effective mass m^* as $\sqrt{4\pi ne^2/m^*}/\epsilon_\infty$. Here, ϵ_∞ is the dielectric constant contributed to by all the higher energy incoherent excitations. The corresponding plasma frequency along the c axis $\omega^*_{p,c}$ can be found from the reflectivity obtained in grazing incidences; as θ_{in} increases to 55° and 75°, a clear dip structure develops around 0.065 eV corresponding to $\omega^*_{p,c}$. By fitting these curves based on the simple Drude model with anisotropic effective masses [13], m^* in the ab plane and along the c axis could be estimated as about 0.2 and $1.0m_e$, respectively, where m_e is the bare electron mass. On the basis of such directional dependence of the effective masses, BiTeI can be treated as a quasi-two-dimensional system.

The Rashba-type spin splitting in BiTeI naturally implies an interesting diversity for the possible intraband or interband optical transitions, which are depicted by vertical arrows in Fig. 1(c) given that E_F is located just above the conduction band minimum. It is worth mentioning that, besides the free carrier excitation (not indicated) and the interband transition defining the optical gap (γ), there should appear at least three more intraband or interband excitations indexed as α, β, and δ, which would be absent without the Rashba splitting. It should be noted that such optical transitions between the bands with different spin angular momenta are allowed owing to the SOI, a principal reason of such spin-split bands.

Figure 1(d) shows the in-plane optical conductivity spectrum for the sample P which has a minimal n value

($\simeq 0.4 \times 10^{19}/\mathrm{cm}^3$) and hence E_F near the conduction band minimum as displayed in Fig. 1(b). Whereas the free carrier excitation (Drude response) is centered at zero energy, there appear four characteristic energies defining the onsets of the optical excitations marked by α, β, γ, and δ. Such optical features reflect the complex nature of the bands near E_F, and we argue that they have one-to-one correspondence with the intraband or interband transitions marked in the band structure by the same indices. In particular, the large energy scale of the features α and β is a direct consequence of the gigantic Rashba effect in this system.

For the sake of better understanding, we investigate how these optical features will vary as n changes or, equivalently, as E_F shifts. In the left panel in Fig. 2, we present the optical conductivity spectra experimentally obtained for three representative samples with varying n, exhibiting systematic variation as a function of n. Here, the Drude response has been subtracted to give $\Delta\sigma_1$ after its fitting based on the Drude model as shown with the open square symbols in Fig. 1(d).

In the right panel, we present the corresponding theoretical spectra obtained from the Kubo formula:

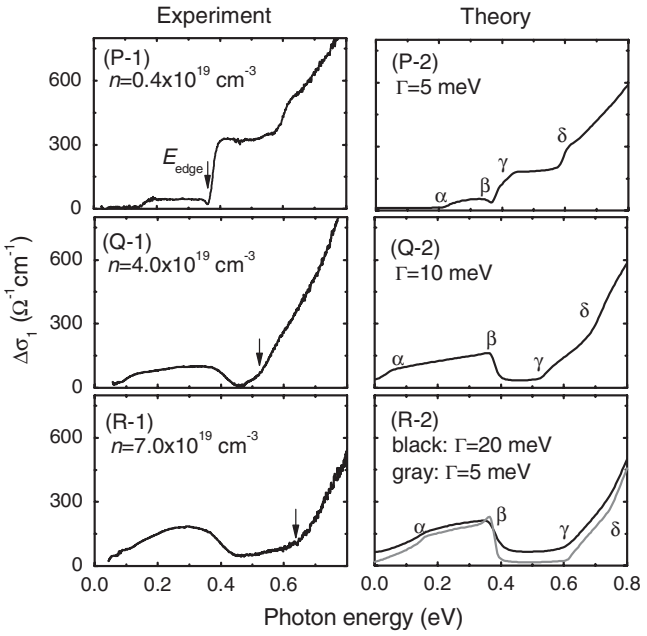

FIG. 2. The comparison between the optical conductivity spectra obtained experimentally (left panels) and theoretically (right panels) for three representative samples with different carrier densities (n) or Fermi levels. All the results are the optical response in the ab plane obtained around 10 K. In the left, the edge of the interband transitions E_{edge} is indicated with arrows. In the right, important spectral features are indexed as $\alpha - \delta$ [see also Fig. 1(b)]. For the sample R, while the curve obtained with $\Gamma = 20$ meV reproduces the experimental result well, the curve with $\Gamma = 5$ meV is also displayed to show the onset features more clearly.

$$\Delta\sigma_1(\omega) = \frac{\hbar e^2}{iV}\sum_{n\neq m}\sum_{\mathbf{k}}\frac{f(\varepsilon_n)}{\varepsilon_m - \varepsilon_n} \times\left(\frac{v_{x,nm}v_{x,mn}}{\varepsilon_m - \varepsilon_n - \hbar\omega} - \frac{v_{x,nm}v_{x,mn}}{\varepsilon_m - \varepsilon_n + \hbar\omega}\right), \quad (1)$$

where $\Delta\sigma_1$ is the incoherent contribution of the optical conductivity, $f(\varepsilon_n)$ is the Fermi-Dirac distribution function, and $\varepsilon_n = \varepsilon_n(\mathbf{k})$ is the eigenenergy corresponding to the nth eigenstate $|n(\mathbf{k})\rangle$. In practice, the energy $\hbar\omega$ needs to be replaced by $\hbar\omega + i\Gamma$ in order to take into account the effect of carrier damping. Here, Γ is assumed to be constant and varied to reproduce the experimental results. The velocity matrix elements $v_{x,nm}$ are defined as

$$v_{x,nm} = \langle n|v_x(\mathbf{k})|m\rangle = \frac{1}{\hbar}\langle n|\frac{\partial H(\mathbf{k})}{\partial k_x}|m\rangle, \quad (2)$$

which is computed by downfolding the *ab initio* Hamiltonian $H(\mathbf{k})$ to an effective low-energy tight-binding model using so-called maximally localized Wannier functions [14–17]. From a previously converged full-potential all-electron calculation done by the WIEN2K package [18], we have accordingly constructed an 18-band tight-binding model for the 12 valence and 6 conduction bands around E_F [19]. In our *ab initio* calculation, the relativistic effects, including the spin-orbit coupling, have been fully taken into account. A detailed description regarding our *ab initio*

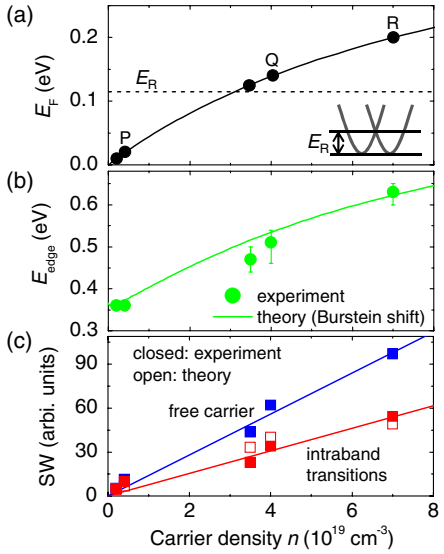

FIG. 3 (color online). (a) The relationship between the position of the Fermi level (E_F) and the carrier density n. E_R corresponds to the Rashba energy defined as the energy difference between the conduction band minimum and the band crossing point as shown in the inset. (b) The optical energy gap (E_{edge}) as a function of n. The solid line corresponds to the expectation of the gap energy based on the Burstein shift. (c) The spectral weight (SW) of the Drude peak and the intraband optical transition, defined between the onsets α and β (see Fig. 2), as a function of n. Solid lines are guides to the eyes.

calculation can be found in Ref. [12]. The effect of carrier doping was treated within the rigid band approximation; the calculated relationship between n and E_F is plotted in Fig. 3(a), where the measured specimens are indicated. Overall, the conductivity spectra obtained theoretically show excellent agreement with the experimental results, while the absolute value in the high energy region above 0.5 eV has been estimated smaller.

Let us discuss the spectral features ($\alpha - \delta$) one after the other, which all are relevant with the Rashba-split bands and revealing the dynamical property of the relativistic electrons. First, the onset γ shows a large shift with the change in n; we estimated its energy E_{edge}, which was found to increase monotonically with n as shown in Fig. 3(b). This behavior can be well explained by the Burstein shift accounting for the shift of E_F to the higher energy with an increase of n [20]. The corresponding energy gap was taken from the band structure as the minimal energy difference between the valence band and E_F with the same wave vector allowing the direct transition. As shown in Fig. 3(b), the energy gap increases monotonically with n, and it connects well the discrete data points experimentally estimated for the five samples.

Second, as a characteristic feature of the interband transitions, there appears another onset δ besides γ; it appears around 0.6 eV for the sample P and shifts to higher energy as n increases similarly with the onset γ, which can be more clearly discerned in the theoretical results. Since E_F for the sample P is located near the band minimum, such sharp features reflect the singular behaviors of the density of relevant states. Whereas the onset γ defining E_{edge}, as aforementioned, is ascribed to the excitation from the upper branch of the Rashba-split valence bands to the Fermi level, the other onset δ corresponds to the excitation from the lower branch of the valence bands. Accordingly, their finite energy difference indicates that the valence bands also experience Rashba-type splitting; the splitting energy amounts to about 0.2 eV confirmed both experimentally and theoretically.

Third, the other important optical feature is the existence of the well-defined and broad excitation located around 0.3 eV below the optical gap excitation. Its lower and higher energy onsets are indexed as α and β, respectively, and they correspond to the *intraband* transitions from the Fermi level to the conduction bands as displayed in Fig. 1(b). We integrated $\sigma_1(\omega)$ to estimate the spectral weight of the intraband transition as well as the Drude peak and found that they both increase with n [Fig. 3(c)]. Such behaviors are consistently understood by the fact that these excitations are related to the Fermi surface of which the area should increase in proportion to n. In particular, the theoretical values for the intraband transitions plotted together show an excellent agreement with the experimental values demonstrating that the huge Rashba interaction can account for the observed spectral weight of the intraband transitions. Another important point for this excitation is that its energy width is the largest for the sample Q. In particular, its edge α is located at the lower energy than for other samples. (The tail of spectral intensity towards zero energy results from the c-axis dispersion of the Rashba-split bands.) This indicates that E_F in this case should be located closer to the band crossing point (Dirac point); when it is located exactly at the crossing point, the feature α should appear at zero energy. Consequently, we can argue that E_F of the samples P, Q, and R are located below, near, and above the band crossing point, respectively, as shown in Fig. 3(a). This clearly demonstrates that the band filling can be easily tuned to control the Fermi level position with respect to the band crossing point.

In this work, we have presented a study on the dynamics of relativistic electrons by optical spectra in BiTeI. Several unique spectral features originating from the spin-split Rashba bands are observed experimentally and explained theoretically based on first-principles calculations. Note also that the skin depth of midinfrared light is around 10–30 μm, and, therefore, distinct intraband transitions observed in this spectral region manifest the bulk nature of the Rashba-type spin splitting in BiTeI.

This research is supported by MEXT Grants-in-Aid No. 20740167, No. 19048008, No. 19048015, and No. 21244053, Strategic International Cooperative Program (Joint Research Type) from Japan Science and Technology Agency, and by the Japan Society for the Promotion of Science (JSPS) through the "Funding Program for World-Leading Innovative R&D on Science and Technology (FIRST Program)," initiated by the Council for Science and Technology Policy (CSTP). G. A. H. S. acknowledges support from MEXT and DAAD.

*Present address: Graduate Program of Photonics and Applied Physics, Gwangju Institute of Science and Technology (GIST), 1 Oryong-dong, Buk-gu, Gwangju 500-712, Republic of Korea.
jsl@gist.ac.kr

[1] A. Manchon and S. Zhang, Phys. Rev. B **78**, 212405 (2008).
[2] A. Chernyshov *et al.*, Nature Phys. **5**, 656 (2009).
[3] I. M. Miron *et al.*, Nature Mater. **9**, 230 (2010).
[4] E. Bauer *et al.*, Phys. Rev. Lett. **92**, 027003 (2004).
[5] E. I. Rashba, Sov. Phys. Solid State **2**, 1109 (1960).
[6] J. Nitta *et al.*, Phys. Rev. Lett. **78**, 1335 (1997).
[7] A. Ohtomo and H. Y. Hwang, Nature (London) **427**, 423 (2004).
[8] N. Reyren *et al.*, Science **317**, 1196 (2007).
[9] K. Arii, M. Koshino, and T. Ando, Phys. Rev. B **76**, 045311 (2007).
[10] K. Ishizaka *et al.*, Nature Mater. **10**, 521 (2011).
[11] C. R. Ast *et al.*, Phys. Rev. Lett. **98**, 186807 (2007).

[12] M. S. Bahramy, R. Arita, and N. Nagaosa, Phys. Rev. B **84**, 041202(R) (2011).
[13] In the Drude model, $\epsilon = \epsilon_\infty + \omega_p^2/(\omega^2 + i\omega/\tau)$, and the fitting parameters used are $(\omega_p, 1/\tau, \epsilon_\infty) = (4250\ \mathrm{cm}^{-1}, 230\ \mathrm{cm}^{-1}, 20)$ for the ab plane and $(1900\ \mathrm{cm}^{-1}, 105\ \mathrm{cm}^{-1}, 12.2)$ for the c axis.
[14] I. Souza, N. Marzari, and D. Vanderbilt, Phys. Rev. B **65**, 035109 (2001).
[15] X. Wang *et al.*, Phys. Rev. B **74**, 195118 (2006).
[16] A. A. Mostofi *et al.*, Comput. Phys. Commun. **178**, 685 (2008).
[17] J. Kunes *et al.*, Comput. Phys. Commun. **181**, 1888 (2010).
[18] P. Belaha *et al.*, WIEN2K package: http://www.wien2k.at.
[19] In our tight-binding model, the band gap is increased slightly by 0.08 eV to coincide with the experimental value 0.36 eV.
[20] E. Burstein, Phys. Rev. **93**, 632 (1954).